

# Structure and dynamics in the complex ion $(\text{UO}_2)_2(\text{CO}_3)(\text{OH})_3^-$

Zoltán Szabó,<sup>\*a</sup> Henry Moll<sup>ab</sup> and Ingmar Grenthe<sup>a</sup>

<sup>a</sup> Department of Chemistry, Inorganic Chemistry, Royal Institute of Technology (KTH), S-10044 Stockholm, Sweden

<sup>b</sup> Institute of Radiochemistry, Forschungszentrum Rossendorf e.V., PO Box 510119, D-01314 Dresden, Germany

Received 25th February 2000, Accepted 13th July 2000

Published on the Web 16th August 2000

The structure and ligand exchange dynamics of the ternary complex  $(\text{UO}_2)_2(\text{CO}_3)(\text{OH})_3^-$  have been investigated by EXAFS and NMR spectroscopy. Very broad signals can be observed in both the  $^{13}\text{C}$  and the  $^{17}\text{O}$  NMR spectra. The EXAFS data show the presence of  $1.3 \pm 0.3$  short uranium–oxygen distances at 2.26 Å, consistent with single bonded hydroxide and  $3.9 \pm 0.6$  distances at 2.47 Å for the other ligands in the first co-ordination shell. There is also evidence for a  $\text{U} \cdots \text{U}$  interaction at 3.90 Å. Based on the EXAFS and NMR data we suggest the presence of three isomers with different bridge arrangements, the dominant one, C, contains 80% of the uranium and the minor ones A and B, 5 and 15%, respectively. The ligand exchange reactions between these isomers are slow. The NMR data indicate that the main reactions involve intramolecular exchanges between isomers with different positions of the non-bridging ligands in A, B and C. We suggest that these take place through water exchange as discussed earlier for other ternary uranium(vi) complexes.

## Introduction

In previous communications we have discussed the structures of isomers and the rate and mechanism of their inter- and intra-molecular ligand exchange reactions in some ternary dioxouranium(vi) aqueous systems.<sup>1,2</sup> In the present study we have made an analysis of the structure and dynamics of the ternary complex  $(\text{UO}_2)_2(\text{CO}_3)(\text{OH})_3^-$ . This is a predominant species in the aqueous uranium(vi)–carbonate system over a broad pH range, provided that the ratio between the total concentrations of  $\text{U}^{\text{VI}}$  and total carbonate is  $>1:1$ , cf. Fig. 1. The complex was first identified by Maya and Begun,<sup>3,4</sup> who determined its equilibrium constant and Raman spectrum. Additional information on the equilibrium constant is found in ref. 5, pp. 318–320. From the stoichiometry of the complex and the known co-ordination geometry of the uranyl ion<sup>6,7</sup> it follows that the two uranium atoms are linked by bridging carbonate and/or hydroxide groups and that the complex also contains co-ordinated water. The four possible isomeric bridging structures are shown in Fig. 2. The  $\text{U} \cdots \text{U}$  distance in A and B can be estimated to be 4.97 and 3.95 Å respectively, from known structures containing these bridge types.<sup>8–10</sup> For each of these there are additional isomers possible, depending on the arrangement of the non-bridging ligands.

In order to decide if different isomers are formed, their structures and possible pathways for their interconversion we have used EXAFS,  $^{13}\text{C}$  and  $^{17}\text{O}$  NMR data from solutions containing  $(\text{UO}_2)_2(\text{CO}_3)(\text{OH})_3^-$ . The NMR data provide structure and symmetry information for the isomers and the rate of exchange, as well as mechanistic ideas for the exchange reaction. The EXAFS data give “instantaneous” structure information, i.e. the superimposed structures of the different isomers.

## Experimental

### Chemicals used, preparation of test solutions

The chemicals used were the same as described in previous studies.<sup>1</sup> An  $^{17}\text{O}$ -enriched uranyl perchlorate stock solution was prepared as described earlier.<sup>1</sup> The test solutions for the  $^{17}\text{O}$  and

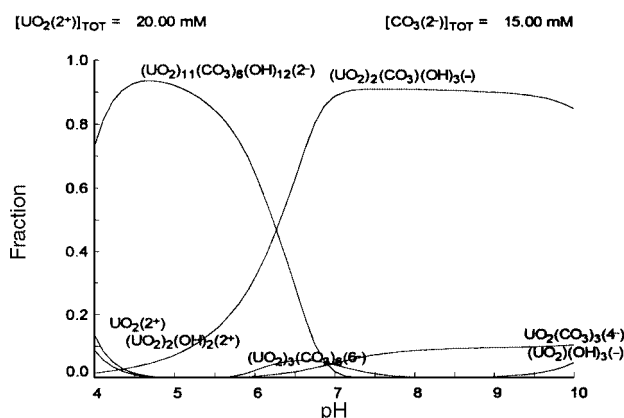


Fig. 1 Uranium distribution diagram for the uranium(vi)–carbonate system as a function of pH.

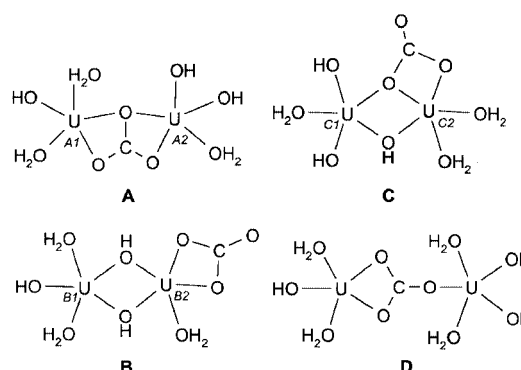
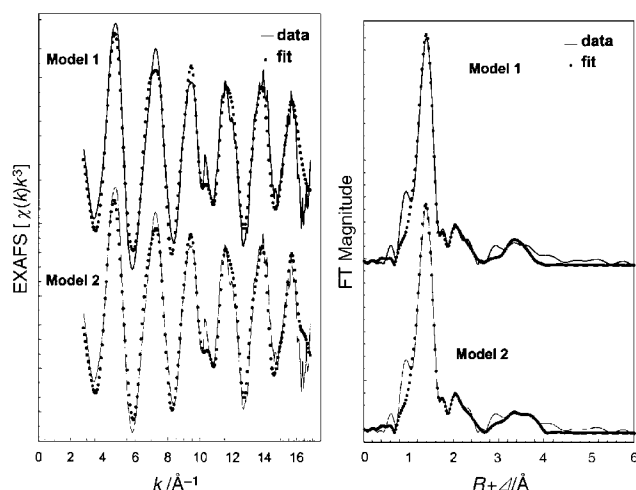


Fig. 2 Possible bridge isomers for  $(\text{UO}_2)_2(\text{CO}_3)(\text{OH})_3^-$ ; ( $\text{U} = \text{UO}_2^{2+}$ ).

$^{13}\text{C}$  NMR experiments were prepared from appropriate amounts of  $^{17}\text{O}$ -enriched uranyl perchlorate stock solution and solid  $^{13}\text{C}$ -enriched  $\text{Na}_2\text{CO}_3$  (Stohler Isotope Chemical, 99.3%  $^{13}\text{C}$ ) to get the final total concentration of 0.02 M  $\text{UO}_2^{2+}$ . First, the ratio of  $[\text{UO}_2^{2+}]:[\text{CO}_3^{2-}]$  in the test solution was set to 1:3 at pH 7.5. This solution contains mainly  $\text{UO}_2(\text{CO}_3)_3^{4-}$ ; argon was then bubbled through the stirred solution and 1 M  $\text{HClO}_4$  was



**Fig. 3** Experimental EXAFS oscillations, corresponding Fourier transforms (using a Bessel window), and best theoretical fits for a sample containing  $\approx 94\%$   $(\text{UO}_2)_2(\text{CO}_3)(\text{OH})_3^-$ .

added dropwise, slowly decreasing the pH to 5 and removing the excess of carbonate. The final ratio of  $[\text{UO}_2^{2+}]:[\text{CO}_3^{2-}]$  was approximately 2:1. It is important to note that the pH cannot be below 4.5 because of precipitation of  $\text{UO}_2\text{CO}_3(\text{s})$ . Then the pH was changed back to the range between 7 and 8 by adding a NaOH solution; this results in the formation of  $(\text{UO}_2)_2(\text{CO}_3)(\text{OH})_3^-$  as the dominant complex. For EXAFS measurements no isotope enriched chemicals were used and the test solution had a total uranium(vi) concentration of 0.05 M, of which about 94%, estimated from  $^{13}\text{C}$  NMR, was  $(\text{UO}_2)_2(\text{CO}_3)(\text{OH})_3^-$ .

### NMR Measurements

The  $^{17}\text{O}$  NMR spectra were measured using 10 mm sample tubes, on a Bruker AM400 spectrometer at 54.2 MHz; the chemical shifts are given in ppm and referenced to the signal of external tap water. The  $^{13}\text{C}$  NMR spectra were measured using 5 or 10 mm sample tubes, on Bruker DMX-500 (11.7 T) and Avance-800 (18.8 T) spectrometers, at 125 and 200 MHz, respectively. The  $^{13}\text{C}$  chemical shifts are referred to external TMS. In the test solutions 5%  $\text{D}_2\text{O}$  was used to obtain locked mode. The probe temperature was adjusted using a Bruker Eurotherm variable temperature control unit and measured by a calibrated Pt-100 resistance thermometer. The linewidths were determined by deconvolution of Lorentzian curves to the experimental signals using the WIN-NMR program.<sup>11</sup>

### EXAFS Measurements

The data were recorded at the Rossendorf Beamline (ROBL) at the ESRF in Grenoble. The transmission spectra were measured at room temperature using a water-cooled Si(111) double-crystal monochromator of fixed-exit type ( $E = 5\text{--}35$  keV). Further details on EXAFS measurements are given in ref. 12. The data were treated using the WinXAS software.<sup>13</sup> Theoretical back-scattering phase and amplitude functions used in the data analysis were calculated for the model complex  $(\text{UO}_2)_2(\text{CO}_3)(\text{OH})_3^-$  using the FEFF7 program.<sup>14</sup> The multiple scattering (MS) path U–O (axial, 4-legged path) and MS U–C–O (3- and 4-legged paths) were included in the model calculations.

## Results

### EXAFS experiments

Each of the possible isomers, cf. Fig. 2, contains two uranium sites with different chemical surroundings. The experimental data record a superposition of all these, i.e. the “average” struc-

**Table 1** Fit parameters to uranium  $\text{L}_{\text{III}}$  edge EXAFS data:  $\Delta E_0$  set at  $-6.6$  eV. Refinements were made using a constant amplitude reduction factor  $S_0^2 = 0.9$

Fit model	Scattering path	$N$	$\sigma^2/\text{\AA}^2$	$R/\text{\AA}$	Residual (%)
1	U–O <sub>ax</sub>	2 <sup>a</sup>	1.80 <sub>9</sub>	0.0017	17.3
	U–O <sub>eq1</sub>	$1.7 \pm 0.3$	2.26 <sub>4</sub>	0.0048	
	U–O <sub>eq2</sub>	$3.5 \pm 0.5$	2.47 <sub>4</sub>	0.0104	
	U–C	$0.9 \pm 0.2$	2.89 <sub>6</sub>	0.0036	
	U–O <sub>ax</sub>	2 <sup>a</sup>	3.61 <sub>9</sub>	0.0035	
	(MS pathway)				
	U–C–O	3 <sup>a</sup>	3.95 <sub>0</sub>	0.0047	
2	(MS pathway)				14.8
	U–O <sub>ax</sub>	2 <sup>a</sup>	1.81 <sub>0</sub>	0.0017	
	U–O <sub>eq1</sub>	$1.3 \pm 0.3$	2.26 <sub>0</sub>	0.0036	
	U–O <sub>eq2</sub>	$3.9 \pm 0.6$	2.47 <sub>0</sub>	0.0130	
	U–C	$1.5 \pm 0.3$	2.89 <sub>1</sub>	0.0056	
	U–U	$0.5 \pm 0.1$	3.90 <sub>3</sub>	0.0036	
	U–O <sub>ax</sub>	2 <sup>a</sup>	3.62 <sub>0</sub>	0.0035	
	(MS pathway)				
	U–C–O	3 <sup>a</sup>	3.96 <sub>0</sub>	0.0053	
	(MS pathway)				

<sup>a</sup> Kept constant during the fit.

ture present in the test solution, a fact that will complicate the EXAFS structure analysis. The experimental data extend out to a  $k$  value around  $16.5 \text{ \AA}^{-1}$  which permitted the resolution of the equatorial bond distances into two components. The EXAFS analysis was made in several steps, beginning with the first co-ordination sphere of uranium, including MS pathways but without a  $\text{U} \cdots \text{U}$  distance, Model 1. Then a calculation of a difference spectrum using the experimental data and the calculated total EXAFS oscillation from Model 1 was made. This allowed the identification of two additional shells at approximately  $3.37$  and  $3.75 \text{ \AA}$ , respectively. In Model 2 it was assumed that the latter distance referred to a U–U interaction. The result of refinements of Models 1 and 2 and a comparison between models and experimental data are given in Table 1 and Fig. 3. There is no large difference between the two models, however both very clearly identify two different uranium–oxygen distances in the equatorial plane. The short distance at  $2.26 \text{ \AA}$  and  $N = 1.3 \pm 0.3$  indicates a co-ordinated single bonded hydroxide, as observed both in the solid state and in solution,<sup>15,16</sup> while the longer distance at  $2.47 \text{ \AA}$  and  $N = 3.5 \pm 0.5$ , indicates bridging hydroxide<sup>8</sup> and co-ordinated carbonate.<sup>9</sup> The number of short distances is important for the deduction of the structures of the main isomers as outlined in the Discussion. The presence of the short U–O<sub>eq1</sub> distance is supported by a significant lengthening of the U–O<sub>ax</sub> bond distance, about  $0.03 \text{ \AA}$ , compared to that of the uranyl aqua ion.<sup>16</sup> The measured bond distance U–O<sub>ax</sub>,  $1.81 \text{ \AA}$ , is also slightly larger than found in the binary complex,  $(\text{UO}_2)_3(\text{CO}_3)_6^{6-}$ ,  $1.79 \text{ \AA}$ .<sup>9</sup> A notable feature in the EXAFS spectrum is the absence of the strong U–U peak found in the EXAFS data<sup>9,17</sup> from  $(\text{UO}_2)_3(\text{CO}_3)_6^{6-}$ ,  $(\text{UO}_2)_2(\text{OH})_2^{2+}$  and  $(\text{UO}_2)_3(\text{OH})_5^+$ . Allen *et al.* made similar observations on dinuclear complexes of tartrate, malate and citrate.<sup>18</sup> The absence of a distinct U–U peak is a strong indication of the presence of at least two isomers in solution with slightly different U–U distances, resulting in a smearing out of the peak in the same manner as caused by a large Debye–Waller factor.

### NMR measurements

Very broad signals can be observed for  $(\text{UO}_2)_2(\text{CO}_3)(\text{OH})_3^-$  in both the  $^{13}\text{C}$  and the  $^{17}\text{O}$  spectra, cf. Figs. 4 and 5, which cannot be due to exchange reactions involving the other species present in the test solution. The  $^{13}\text{C}$  and  $^{17}\text{O}$  linewidths of  $\text{UO}_2(\text{CO}_3)_3^{4-}$  and  $(\text{UO}_2)_3(\text{CO}_3)_6^{6-}$ , which are present in low concentrations, are narrow indicating very slow exchange between one another and with  $(\text{UO}_2)_2(\text{CO}_3)(\text{OH})_3^-$ . The line broadening of the free

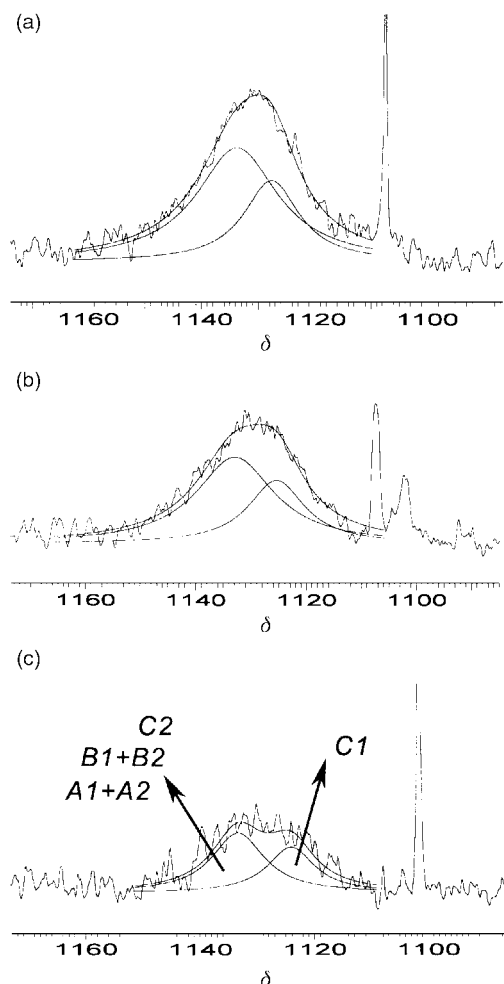
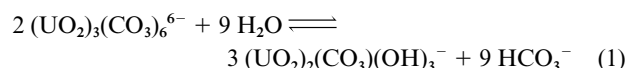


**Fig. 4**  $^{17}\text{O}$  NMR spectra for  $(\text{UO}_2)_2(\text{CO}_3)(\text{OH})_3^-$  and deconvoluted peaks for the “yl” oxygens within the isomers (see Fig. 2 and text). The spectra were measured at different pH, a 7.0, b 7.4 and c 8.3 at 25 °C. The sharp peaks at  $\delta$  1102 and 1108 are for  $\text{UO}_2(\text{CO}_3)_3^{4-}$  and  $(\text{UO}_2)_3(\text{CO}_3)_6^{6-}$ , respectively.

bicarbonate is due to proton exchange, in accordance with the result of a recent study on the dynamics of intra- and intermolecular exchange reactions in binary carbonate complexes.<sup>19</sup> Hence, the only explanation for the broad signals is an intramolecular exchange between different isomers with the same bridging ligands. In the carbon spectrum recorded at 11.7 T (125 MHz) two narrower peaks of low intensity can be deconvoluted beside the broad (240 Hz) main peak. The relative intensities of these are 15 and 5%, as shown in Fig. 5. It was not possible to resolve the broad carbon peaks either by decreasing the temperature, or by increasing the magnetic field to 200 MHz, *cf.* Discussion. In both experiments the linewidth was increasing. In addition we found that the concentration of  $(\text{UO}_2)_2(\text{CO}_3)(\text{OH})_3^-$  decreased significantly when decreasing the temperature, indicating that the enthalpy change for reaction (1)



is positive as expected when nine  $\text{CO}_3^{2-}$  (co-ordinated) react with the equivalent amount of water to give  $\text{OH}^-$  (co-ordinated) and  $\text{HCO}_3^-$ .

The  $^{17}\text{O}$  NMR spectra measured at different pH are shown in Fig. 4. The broad peak indicates the presence of at least two different uranium sites in slow exchange. The peak can be deconvoluted into two broad Lorentzian curves with a ratio of approximately 1.5:1. The peak is broadening and its intensity is decreasing when decreasing the temperature to 0 °C and it is

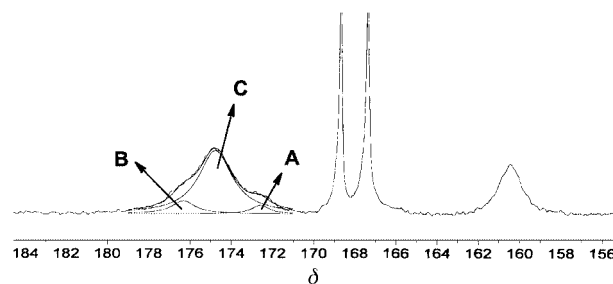


**Fig. 5**  $^{13}\text{C}$  NMR spectrum measured at 125 MHz for  $(\text{UO}_2)_2(\text{CO}_3)(\text{OH})_3^-$  (pH 7.0, 25 °C). The arrows indicate the deconvoluted peaks for the isomers (see Fig. 2). The peaks at  $\delta$  168.8, 167.2 and 160.2 are for  $(\text{UO}_2)_3(\text{CO}_3)_6^{6-}$  (in central and terminal positions) and  $\text{HCO}_3^-/\text{CO}_3^{2-}$  respectively.

then not possible to detect individual peaks. The shift difference between the two peaks is approximately 500 Hz, which can be used as an upper limit for the rate of exchange between the uranyl sites at 25 °C.

## Discussion

From the experimental data it was only possible to deduce structure models for the different bridge isomers of  $(\text{UO}_2)_2(\text{CO}_3)(\text{OH})_3^-$ . Hence, the mechanism for the intramolecular exchange reaction is tentative.

The first step in the analysis is to consider the relative stability, the structure and dynamics of the bridge isomers shown in Fig. 2. From there on we will continue with a discussion of the possible additional isomers that differ in the positions of the non-bridging ligands.

## EXAFS data

The different bridge isomers differ in their  $\text{U} \cdots \text{U}$  distances and in the number of non-bridging  $\text{OH}^-$  groups. The  $\text{U} \cdots \text{U}$  distances in the different bridges have been estimated from known structures, 3.90 Å in  $^8 (\text{UO}_2)_2(\text{OH})_2^{2+}$ , 4.90 Å in A, based on the known structure<sup>9</sup> of  $(\text{UO}_2)_3(\text{CO}_3)_6^{6-}$ . The  $\text{U} \cdots \text{U}$  distance in D is estimated from the geometry to be 6.6 Å. A key point for the analysis is the possibility to identify the number of terminal OH groups from the EXAFS data. The EXAFS models indicate  $1.3 \pm 0.3$  short U–O distances per uranium. In addition the best model has  $0.5 \pm 0.1$   $\text{U} \cdots \text{U}$  distances per uranium at 3.90 Å. This leaves C as the model most consistent with the EXAFS data.

The next issue is to judge if the observed exchange is due to exchange between the different bridge isomers, or if it is a result of exchange between the non-bridging ligands. Experimental kinetic information indicates that bridging ligands are not particularly reactive. The rates of formation and dissociation of  $(\text{UO}_2)_2(\text{OH})_2^{2+}$  are slow,  $k_f \approx 60 \text{ s}^{-1}$  and  $k_d \approx 100 \text{ s}^{-1}$ , respectively.<sup>20</sup> The rate of dissociation of  $(\text{UO}_2)_3(\text{CO}_3)_6^{6-}$ , containing the same double bridging carbonate as in A, is  $\approx 1 \text{ s}^{-1}$ . In addition, the exchange between different bridge isomers involves a major rearrangement and is therefore less likely than reactions involving the non-bridging ligands.

## The relative stability of the different isomers

We have no quantitative information of this type. However, the NMR data indicate that the exchanging isomers must be present in comparable amounts, *i.e.* their relative stability cannot differ more than a factor of five at most. We expect that the difference in thermodynamic stability between isomers with different bridge structures is larger than between isomers with the same bridge structure, as observed experimentally for other ternary uranium(VI) complexes.<sup>1</sup> The experimental information from the  $^{13}\text{C}$  data, indicating 80% of isomer C, and 5 and 15% of A and B, respectively, is consistent with this assumption. If

we compare isomers A and D we note that the bonding capacity of the carbonate ion is used less efficiently in D than in A, accordingly D is not likely to be present in significant amounts in the test solutions.

### <sup>17</sup>O and <sup>13</sup>C NMR experiments

The deconvolution of the carbon spectrum indicates the existence of at least 3 bridging isomers. The peak at  $\delta$  172.5 has been assigned to isomer A because this is the narrowest (110 Hz), *i.e.* belonging to the slowest exchange reaction, which we expect involve the double bridging carbonate. The peak at  $\delta$  176.2 with a linewidth of 160 Hz is then due to the other minor component, B. The line broadening is not due to exchange between the bridging isomers; the rate of exchange calculated from the measured linewidth and population should then be the same.<sup>21</sup> This is not the case; instead the line broadening is due to a more rapid exchange of the non-bridging ligands. In isomer B the carbonate is in terminal position and we can assume a much faster intermolecular exchange, as was observed in binary<sup>19</sup> and ternary<sup>1</sup> carbonate systems. At the experimental pH (7.0) we estimate an external carbonate exchange rate of 230 s<sup>-1</sup>, using the rate constant ( $2.3 \times 10^9$  M<sup>-1</sup> s<sup>-1</sup>) for the proton catalysed exchange in the binary carbonate system.<sup>19</sup> This value is lower than that calculated from the linewidth (460 s<sup>-1</sup>), which indicates the effect of the exchange of other non-bridging ligands on the line shape. The major peak at  $\delta$  175 is assigned to bridge isomer C. The additional isomers with the same bridge structure should have approximately the same thermodynamic stability, *cf.* ref. 1, but different <sup>13</sup>C chemical shifts. The simplest exchange reaction involves site exchange of water and hydroxide around uranium site C1. We have previously studied<sup>1</sup> reactions of this type between isomers of UO<sub>2</sub>(ox)F<sub>2</sub>(H<sub>2</sub>O)<sup>2-</sup> and UO<sub>2</sub>(ox)F(H<sub>2</sub>O)<sub>2</sub><sup>-</sup>, and found that their rate constants, approximately 1500 s<sup>-1</sup>, are determined by the rate of dissociation of co-ordinated water. We expect that the rate of exchange of water to be similar also in C.

The deconvoluted <sup>17</sup>O spectra indicate two different major uranium sites, with the ratio 1.5:1. Owing to the limited resolution of the spectra more exchanging sites cannot be resolved. The <sup>17</sup>O spectra can be explained as follows: in all isomers there are two uranyl oxygen sites in different chemical environments (A1–A2, B1–B2 and C1–C2, see Fig. 2). The chemical shift difference between them is determined by their chemical surroundings, especially the position of carbonate. For the different isomers of C, we can therefore assume that the chemical shift difference between sites C1 and C2 is relatively large and that the exchange between them is slow because of slow carbonate exchange. However, the intensity of the two <sup>17</sup>O peaks is not identical as required if only isomers of C contribute. About 15% of the uranium is contained in isomer B and will therefore give a corresponding contribution to the <sup>17</sup>O spectrum. When discussing the <sup>13</sup>C spectra we pointed out that the carbonate exchange in B was faster than in C. This will result in an exchange averaged <sup>17</sup>O peak from B1 to B2; we suggest that this overlaps the peak at  $\delta$  1132 from isomer C. The ratio of the two <sup>17</sup>O peaks is then 1.4:1, close to the experimental value of 1.5:1. The linewidth of the <sup>13</sup>C and <sup>17</sup>O NMR signals increases with decreasing temperature (or increasing magnetic field). If the peak width is a result only of intermolecular exchange of carbonate we expect a decrease of the linewidth with decreasing temperature because these exchanges are slow on the NMR timescale, even at room temperature. The observed line broadening is then due to slower exchange reactions of the non-bridging ligands with decreasing temperature. These are in the fast exchange region on the NMR timescale at room temperature, resulting in only one peak for each of the bridge isomers. Hence, a decrease of the temperature results in a broadening of the NMR lines.

To conclude, the constitution of this chemical system is

simple, however, the presence of different isomers of (UO<sub>2</sub>)<sub>2</sub>-(CO<sub>3</sub>)(OH)<sub>3</sub><sup>-</sup> complicates both the determination of the structure of the complexes and the understanding of the mechanisms of transformation between them. The NMR line shapes reflect the effects of slow and fast ligand exchanges. The carbonate exchange reactions are relatively slow and make it possible to deconvolute separate <sup>13</sup>C peaks for the isomers and separate <sup>17</sup>O peaks for the major isomer C. Nevertheless, the presence of isomers due to the non-bridged ligands and their internal site exchange reactions are fast on both the <sup>17</sup>O and <sup>13</sup>C NMR timescales determined by the chemical shifts resulting in additional broadening for the signals. Based on EXAFS and NMR data we suggest that there is one predominant bridge isomer, C, and two minor ones, A and B. The predominant exchange reaction in C is an intramolecular exchange between isomers with different positions of the non-bridging ligands. The exchange between them may take place through water exchange as discussed in one of our previous papers.<sup>1</sup>

### Acknowledgements

The experimental work (EXAFS) was supported by the European Commission within the Training and Mobility of Researcher (TMR) Program under contract number ERBFMBICT972296. The authors thank Tobias Reich, Christoph Hennig and Andre Rossberg (Forschungszentrum Rossendorf, Dresden, Germany) for their help during the EXAFS measurements at ROBL (ESRF). Károly Micskei (KLTE, Debrecen, Hungary) is also thanked for making some preliminary <sup>13</sup>C NMR measurements.

### References

- 1 Z. Szabó, W. Aas and I. Grenthe, *Inorg. Chem.*, 1997, **36**, 5369.
- 2 Z. Szabó and I. Grenthe, *Inorg. Chem.*, 1998, **37**, 6214.
- 3 L. Maya and G. M. Begun, *J. Inorg. Nucl. Chem.*, 1981, **43**, 2827.
- 4 L. Maya, *Inorg. Chem.*, 1982, **21**, 2895.
- 5 I. Grenthe, J. Fuger, R. J. M. Konings, R. J. Lemire, A. B. Muller, C. Nguyen-Trung and H. Wanner, *Chemical Thermodynamics of Uranium*, North-Holland, Amsterdam, 1992.
- 6 A. F. Wells, *Structural inorganic chemistry*, Clarendon Press, Oxford, 5th edn., 1984.
- 7 I. Farkas, I. Bányai, Z. Szabó, U. Wahlgren and I. Grenthe, *Inorg. Chem.*, 2000, **39**, 799.
- 8 M. Åberg, *Acta Chem. Scand.*, 1969, **23**, 791.
- 9 P. G. Allen, J. J. Bucher, D. L. Clark, N. M. Edelstein, S. A. Ekberg, J. W. Gohdes, E. A. Hudson, N. Kaltsoyannis, W. W. Likens, M. P. Neu, P. D. Palmer, T. Reich, D. K. Shuh, C. D. Tait and B. D. Zwick, *Inorg. Chem.*, 1995, **34**, 4797.
- 10 M. Åberg, D. Ferri, J. Glaser and I. Grenthe, *Inorg. Chem.*, 1981, **22**, 3981.
- 11 WIN-NMR, Version 6.0, Bruker-Franzen Analytik GmbH, Reinsteffen, Federal Republic of Germany.
- 12 W. Matz, N. Schell, G. Bernhardt, F. Prokert, T. Reich, J. Claußner, W. Oehme, R. Schlenk, S. Dienel, H. Funke, F. Eichhorn, M. Betzl, D. Pröhl, U. Strauch, G. Hüttig, H. Krug, W. Neumann, V. Brendler, P. Reichel, M. A. Denecke and H. J. Nitsche, *J. Synchrotron Rad.*, 1999, **6**, 1076.
- 13 T. Ressler, *J. Synchrotron Rad.*, 1998, **5**, 118.
- 14 S. I. Zabinsky, J. J. Rehr, A. Ankudinov, R. C. Albers and M. Eller, *J. Phys. Rev. B*, 1995, **52**, 2995.
- 15 D. L. Clark, S. D. Conradson, R. J. Donohoe, W. Keogh, D. E. Morris, P. D. Palmer, R. D. Rogers and C. D. Tait, *Inorg. Chem.*, 1999, **38**, 1456.
- 16 U. Wahlgren, H. Moll, I. Grenthe, B. Schimmelpfennig, L. Maron, V. Vallet and O. Groen, *J. Phys. Chem. A*, 1999, **103**, 8257.
- 17 H. Moll, T. Reich and Z. Szabó, *Radiochim. Acta*, in press.
- 18 P. G. Allen, D. K. Shuh, J. J. Bucher, N. M. Edelstein, T. Reich, M. A. Denecke and H. Nitsche, *Inorg. Chem.*, 1996, **35**, 784.
- 19 I. Bányai, J. Glaser, K. Micskei, I. Tóth and L. Zékány, *Inorg. Chem.*, 1995, **34**, 3785.
- 20 W. S. Jung, M. Harada, H. Tomiyasu and H. Fukutomi, *Bull. Chem. Soc. Jpn.*, 1988, **61**, 3895.
- 21 Z. Szabó and J. Glaser, *Magn. Reson. Chem.*, 1995, **33**, 20.